RESEARCH ON OPTIMAL DESIGN OF SPUDCAN STRUCTURES TO EASE SPUDCAN-FOOTPRINT INTERACTIONS IN CLAY AND COMPARATIVE ANALYSES WITH DIFFERENT MEASURES

Huafeng Yu[1]
Zhenzhou Sun[1]
Linlin He*[1, 2]
Liu Yang[2]

[1] Key Laboratory of Far-shore Wind Power Technology of Zhejiang Province, China

[2] National Engineering Research Center for Inland Waterway Regulation, Chongqing Jiaotong University, China

* Corresponding author: *helinl@126.com (L. He)*

ABSTRACT

In order to ease consequences of spudcan-footprint interactions during jack-up rigs reinstalling in the vicinity of an existing seabed footprint, three new types of spudcan shapes, that is, a lotus-shaped spudcan with six circular holes, a flat-bottomed spudcan, and a concave-shaped spudcan, were proposed to perform an optimizing study of the spudcan structures, and the effectiveness of them were analyzed comparatively with other different measures. Firstly, 3D Large Deformation Finite Element (LDFE) analyses were carried out using the Coupled Eulerian-Lagrangian (CEL) method in the commercial finite element package ABAQUS. After calibrating the validity of the numerical calculation model against existing centrifuge test data and LDFE results, the differences in interaction mechanism between the novel spudcans and the generic spindle-shaped spudcan were studied when penetrating near an existing footprint with an eccentric distance of 0.5D, and the horizontal range of plastic deformation of the disturbed soils, the inclination angle of the spudcan and the offset distance of the pile legs were analyzed comparatively as well. The results show that the proposed novel spudcans can mitigate the maximum horizontal sliding force and the maximum bending moment at the top of the pile leg obviously, compared with those of the generic one, which were reduced by 32.59%, 22.47%, 28.18%, and 26.32%, 12.88%, 18.02%, respectively. It also can be seen that all novel structures can ease the adverse consequences of spudcan-footprint interactions effectively, and can improve the in -place stability of the spudcan as well. Finally, three possible measures in mitigating interactions of the spudcan-footprint were contrasted, that is, the novel spudcan (represented by the lotus-shaped spudcan with six holes), stomping method, and perforation drilling method. The results show that all of them can reduce adverse impacts induced by interactions of the spudcan-footprint, and also can improve the in-place stability of the spudcan during reinstallation. In addition, among them, according to the effect of reducing the additional stress of the spudcan, the effectiveness of them can be listed as follows: perforation drilling near an existing footprint > the lotus-shaped spudcan with six holes > stomping method. In terms of the vertical bearing capacity of the spudcan, the lotus-shaped spudcan with six holes can improve it as much as 16.33% compared with the spindle-shaped structure due to the particularity of the structure. While reducing the continuity and strength of soil foundations, the perforation drilling measure leads to the decrease of the vertical bearing capacity of the spudcan by 13.07%. It can be concluded that all the three measures have merits and demerits, so the relevant construction environment conditions and engineering practice should be fully considered when selecting measures to deal with interactions of the spudcan-footprint.

Keywords: Spudcan-footprint interaction,novel spudcan shape,VHM curves,stomping,perforation drilling

INTRODUCTION

Mobile self-elevating jack-up rigs are commonly employed for oil, gas and wind power exploration and exploitation in shallow to moderate water depths (≤150m) due to their proven characteristics, such as flexibility, mobility and cost-effectiveness [1-2]. Most jack-up rigs typically consist of a buoyant triangular or rectangular platform supported by three or four independent pile legs, and each of them is fixed to a large-diameter spudcan. After the completion of offshore drilling, the pile legs will be retracted from the seabed, leaving depressions, which are generally referred to as a crater, or footprint, at the site.

With the development of offshore resources, the jack-up rigs are usually required to be reinstalled in or next to a previous footprint to service the existing wells, drill additional new wells, or install jackets or wind turbines [3]. However, owing to the existence of footprint in the seabed and non-uniform soil strength profiles, it has been proved rather hazardous due to a high potential for the spudcan to slide towards the center of the footprint, and then leading to a failure to install the platform in the required position, or even bumping into the adjacent operating jacket platform, as shown in Fig. 1 [4]. With escalating demand for jack-up rigs to return to the built-up area to perform tasks, instability accidents of offshore platforms induced by spudcan-footprint interactions are subsequently rising dramatically [5]. The frequency of this kind of offshore incidents has increased by a factor of four between the period of 1979~1988 and 1996~2006 [6], even at a higher rate from 2005 to 2012 [7]. Actually, the spudcan-footprint interaction when reinstalling near an existing footprint has been recognized as the second most frequent reason for the geotechnical failure of jack-up rigs [8]. Besides, according to the statistics of Berg, offshore operations of Shell EP company have left approximately 1200 depressions or craters on the seabed, leading to about 80 new wells adjacent to the existing footprints formed by craters every year [9]. Therefore, it is imperative to further investigate mechanical behaviors of jack-up rigs during installing near an existing footprint and seek feasible measures to reduce adverse consequences induced by spudcan-footprint interactions.

To solve this issue, phenomena and consequences induced by spudcan-footprint interactions have been investigated by many researchers [4,5,10-12]. In terms of footprint geometry, the results of centrifuge tests showed that a conical footprint with depth $z_F = (0.22 - 0.33)D$ (D is the diameter of the spudcan) was formed in soft clay, while a cylindrical footprint with depth $z_F = (0.50 - 0.66)D$ was formed in stiff clay. In addition, due to the complexity of the soil flow mode during the process of penetrating and extracting, the total width of the footprint has been proven to be approximate $(1.92 - 1.96)D$. Schematic diagrams of a typical conical footprint in clay are shown in Fig. 2. And the critical footprint depth of $z_F = 0.33D$ and width of $D_F = 2D$ were considered in this study. Besides, the critical offset ratio λ (defined as $\lambda = \beta / D$, where β is the distance between the footprint centre and the spudcan centre) was identified as 0.5-1. In this paper, the critical offset ratio λ was set as 0.5 to carry out the following research. Due to the complexity and variety of possible strength gradients around the footprint, the foundation with the intact soil strength profile was considered herein. This allows a consistent evaluation of the benefits of the spudcan structures and allows comparative analyses with different measures more reasonable.

In addition, for mitigating spudcan-footprint interactions, a series of mitigating measures have been presented, including stomping [13], reaming [14], infilling [15], successive leg repositioning [16], and water jetting with spudcan preloading [17]. However, the results of the above-mentioned measures have turned out to be either unsatisfactory or inconvenient and uneconomical [18]. Consequently, Hossain et al. [3] and Jun et al. [19] focused on adjusting spudcan structures to alleviate spudcan-footprint interactions and proposed a novel spudcan shape with a flat base and 4 holes, which is based on the mechanism that the flat base can reduce the induced horizontal force and holes can provide a preferential soil flow path to facilitate the spudcan penetrating vertically. The results have initially showed that this measure has a remarkable effect in easing spudcan-footprint interactions.

This paper attempts to further discuss the adjustment of spudcan structures and comparatively analyzes and assesses existing different measures in mitigating spudcan-footprint interactions. The research results of this paper can provide references for related design in offshore engineering.
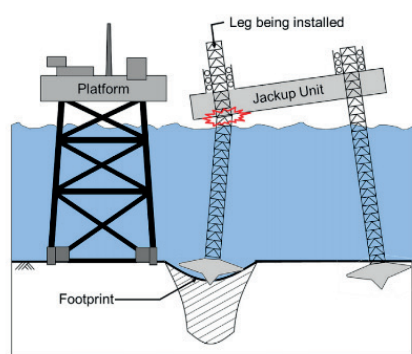

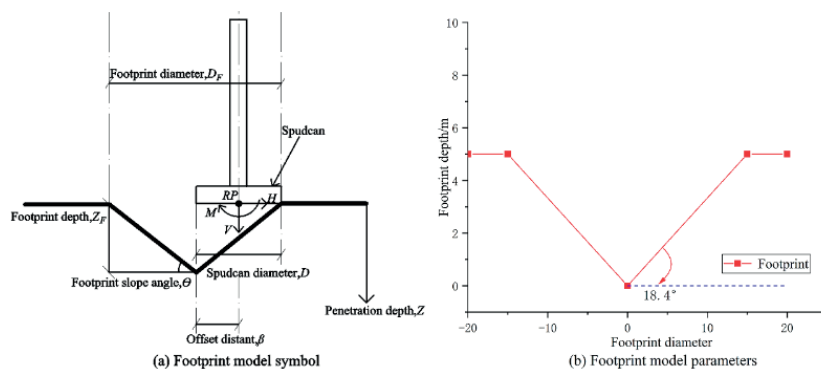*Fig. 1. Schematic diagram of spudcan-footprint interaction*

Fig. 2. Schematic diagram of a conical footprint in clay

NUMERICAL SIMULATION METHOD

During spudcan installing or reinstalling, large deformations of soils are remarkable in the process of penetrating and extracting. 3D Large Deformation Finite Element (LDFE) analysis methods, which are performed by the Coupled Eulerian-Lagrange (CEL) approach in the commercial package ABAQUS/Explicit [21], have been proved suitable to solve geotechnical problems in offshore geotechnical engineering and have been already adopted extensively by many researchers [22-26]. The CEL approach could effectively avoid mesh distortion in LDFE analyses. and the interactions between the spudcan and soil are considered by a contact algorithm called *general contact* in ABAQUS in the process of simulation.

NUMERICAL MODEL OF SPUDCAN-FOOTPRINT INTERACTION

As mentioned above, the CEL approach was adopted to carry out related research on mechanical characteristics of spudcan-footprint interactions. Because of the symmetry of the geometry structure and loading conditions, only half of the spudcan model and the soil model were built to perform related studies. To avoid boundary effects as discussed in preliminary convergence studies and considered by Zheng et al. (2015) [24-25] and Hu et al. (2015) [26], the width of the soil foundation domain from the center of the footprint to the left and right sides of the model were 4D respectively, and the depth of the soil domain was 4D as well. Besides, void elements with the thick of 4m were established above the soil surface to accommodate soils flowing into the empty Eulerian elements to simulate soil heaving and backflow, and an idealized artificial conical footprint was recognized in clay based on research results of Kong et al. (2013)[11], with the diameter $D_f = 2D$ and the depth $Z_F = 0.33D$.

In the model, the soil was discretised as Eulerian elements and the spudcan structure was discretised as Lagrange elements, and the Eulerian mesh included the original soil domain and an overlying layer initially filled with void material. The global soil foundation model is shown in Fig. 3, and its corresponding mesh model is shown in Fig. 4, details of mesh are shown in Fig. 5. In the model, the soil strengths along and adjacent to the footprint were considered to be identical to these of the intact soil, and the rationality and feasibility of which were discussed and confirmed by Jun (2019) [19]. In terms of boundary conditions, the bottom of the soil foundation model was fixed constraint in all the directions, the periphery of the model except for the symmetry surface was constrained in the horizontal direction, and the symmetry surface was set as symmetry constraint. And structuralization hexahedral elements were used to mesh the soil foundation model and linear reductive integral elements C3D8R were used to mesh the spudcan model.
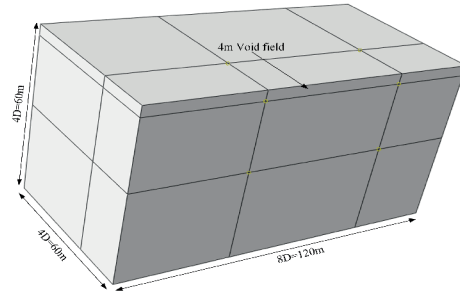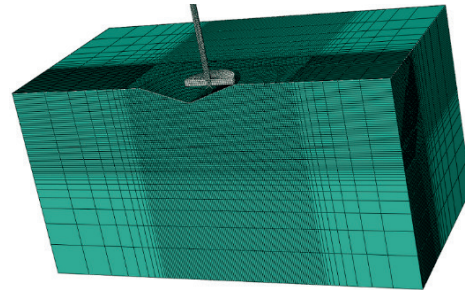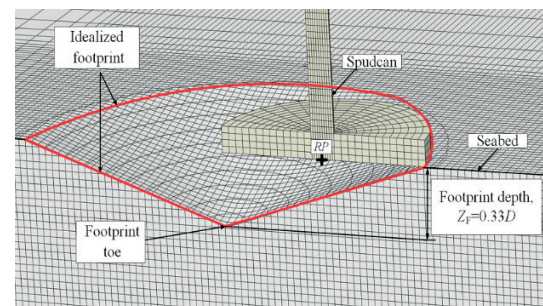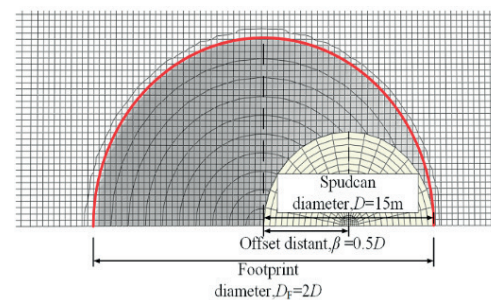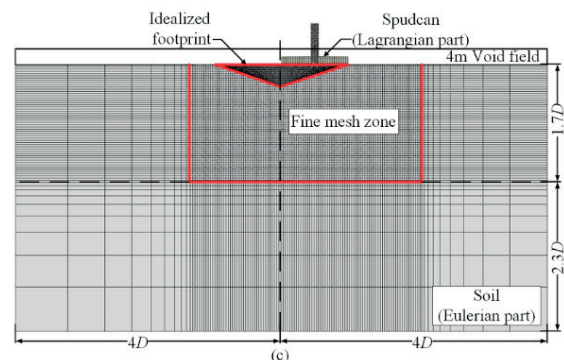

Fig. 3. Sizes of soil foundation

Fig. 4. Mesh model of spudcan and foundation

Fig. 5. Details of mesh of spudcan and foundationNUMERICAL MODEL

CALIBRATION

To ensure subsequent analyses correct, the numerical calculation model built herein was firstly calibrated against previously published literature, including centrifuge test data obtained by Kong et.al. [11] and LDEF results using RITSS (Remeshing and Interpolation Technique with Small Strain) performed by Zhang et.al. [27] and using CEL performed by Jun et.al. [4].In the model, properties of soil material are listed in Table 1, other relative parameters of the model are the same as [4],[11] and [27].

Tab. 1. Properties of soil materials

Parameters	Value
Effective unit weight $\gamma/(KN \cdot m^{-3})$	6.82
Friction angle φ (°)	0
Dilation angle ψ (°)	0
Undrained shear strength s_u / kPa	$\begin{cases} S_u = 7.5 + 0.92 \times z(kPa); 0 \leq z \leq 3.4m \\ S_u = 5 + 1.68 \times z(kPa); z > 3.4m \end{cases}$
Elastic modulus E / kPa	$500s_u$
Poisson's ratio ν	0.49

The soil constitutive adopted in this study was based on an ideal elasto-plastic model and the Tresca strength criterion. The contact between the spudcan and the soil was defined as the master-slave surfaces contact according to the Coulomb's law of friction. In the tangential direction, the friction formula was defined by "penalty function" for the surface between the spudcan and the soil, and in the normal direction it was set as "hard contact".

CALIBRATION AGAINST CENTRIFUGE TESTS AND LDFE ANALYSES

As shown in Fig. 6, it can be seen that the trends of VHM (Vertical reaction force V, horizontal sliding force H, bending moment M) results of this paper and the previous research are the same, but the centrifuge test data are lightly lower than those of other methods. The reason is that, for the centrifugal test, the soils backfill into the footprint or backflow more quickly due to the softening of soils, which leads to the decrease rate of the horizontal force of the spudcan after reaching the peak faster than those calculated by FEM, but the ideal elasto-plastic soil constitutive model adopted in this paper fails to capture the softening effect of the soil in the analyze. However, when the spudcan penetrates to a certain depth in the soil, the results from all the above methods approach the approximate constant value eventually, which verifies the correctness of the CEL calculation model established in this paper.

In addition, due to the complexity of spudcan-footprint interactions, there are only a few studies on the influence of different values of the friction coefficient between the spudcan and the soil on the calculation results currently, and the values of the structure-soil friction coefficient of the calculated models are usually setting as 0.1-0.5 [27-30]. In this paper, the friction coefficients were set as 0.1 and 0.5 respectively to calibrate the numerical calculation model. Although the results when the friction coefficient was set as 0.1 showed closer to those observed in laboratory experiments, the two trends were the same, and Yu [30] has given a conclusion that when the friction coefficient was above 0.5, the values of V, H and M are little affected by the friction coefficient. Therefore, it was set as 0.5 in the subsequent study to ignore the influence of the different friction coefficients on the calculation results.
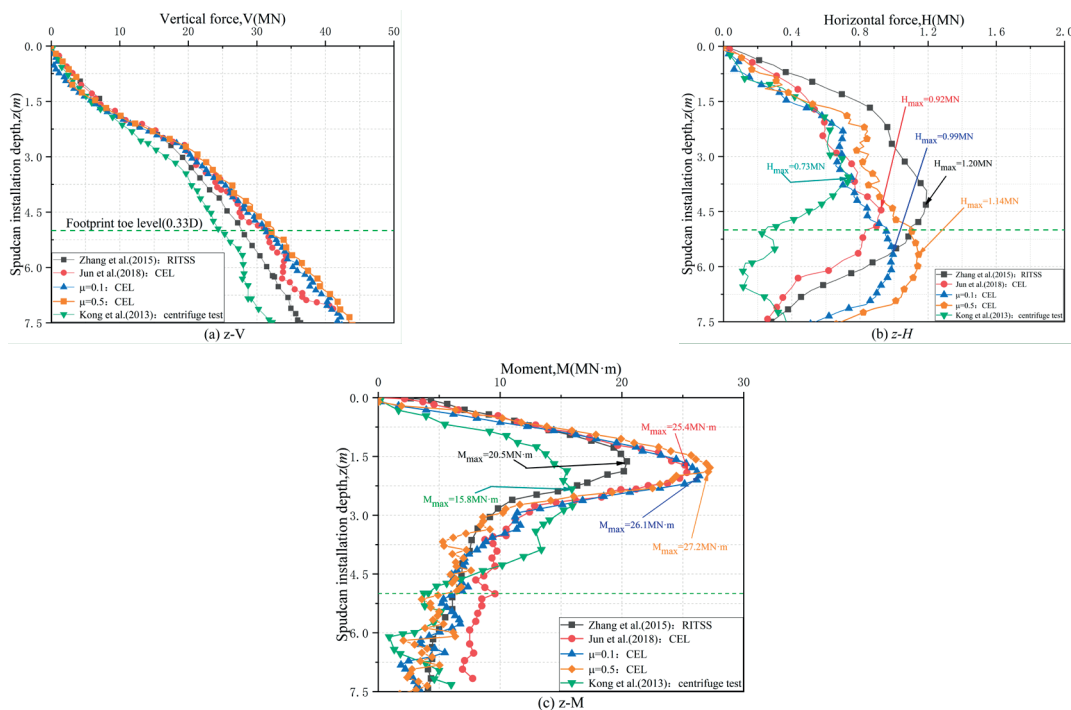

Fig. 6. Numerical model calibration against centrifuge tests and LDFE analyses

OPTIMIZATION MECHANISM OF THE NOVEL SPUDCAN

FAILURE MECHANISM OF SPUDCAN DURING REINSTALLING NEAR THE EXISTING FOOTPRINT

The mechanical characteristics of the traditional spindle-shaped spudcan during penetrating next to an existing footprint are shown in Fig. 7. It can be seen that, due to the obvious asymmetry of soil foundations on both sides of the spudcan, the vertical reaction force of soil acting on the bottom of the spudcan generates an eccentric effect with the eccentric distance e, and a horizontal sliding force H caused by the soil squeezing effect on the right side of a spudcan. Therefore, if the reference point RP of the spudcan is set as shown in Fig. 7, then the spudcan is subjected to a combination of vertical reaction force V, horizontal sliding force H and bending moment with a value of $M = e*v$. In practical engineering, buckling failure of the pile leg below the platform usually occurs as shown in Fig.1. But it has been shown that the combined loadings acting at the reference point RP are not large enough to lead to such an accident. While if the reference point is located on the top of the pile leg, that is, at the point of RP_1, then the mechanical mechanism of the whole pile leg is shown in Fig. 8. It indicates that although the vertical reaction force V and the horizontal sliding force H of the pile leg have not changed with the alteration of the reference point location, there is a much larger amount additional bending moment generates at the reference point RP_1 due to the existence of the horizontal sliding force arm L (the length of the pile leg) , with the value of $M_a = L*H$. Then the total bending moment at the point of RP_1 will be $M_t = M_a + M$, and this value is sufficient to cause structural instability in practice engineering. Besides, the inclination angle of the spudcan α and the offset distance of the pile leg δ induced by the interaction of the spudcan-footprint are shown in Fig. 9. To manifest the variation trend of the spudcan and the pile leg more intuitively, two normalized parameters named the relative inclination angle of the spudcan $\alpha = \tan^{-1}(H/V)$ and the offset distance of pile legs $\delta = M_t/V$ are introduced. The positive horizontal sliding force represents the force of the spudcan sliding towards the footprint, and the positive bending moment represents the counterclockwise bending moment caused by the right side of the spudcan touching the soil firstly.
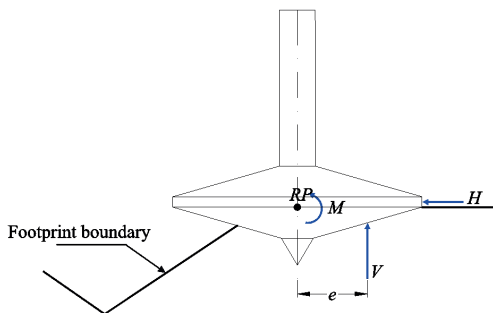

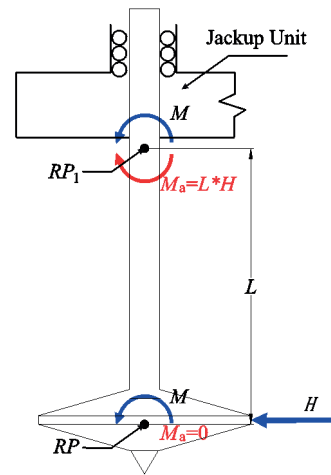Fig. 7. Mechanical characteristics of spudcan during reinstallation

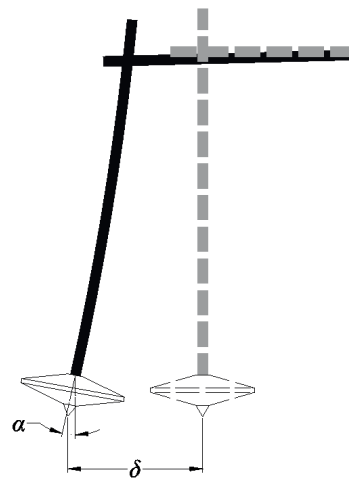Fig. 8. Failure mechanism diagram of pile leg

Fig. 9. Diagram of α and δ

DESIGN BASIS OF OPTIMIZING THE NOVEL SPUDCAN

As shown in Fig. 8, the lowering of horizontal force H on the right side of the spudcan can reduce M_a obviously and then mitigate the sliding risk of the spudcan effectively. However, the resistance of the soil foundation is perpendicular to the bottom surface of the cone during the spindle-shaped spudcan penetrating next to an existing footprint, as shown in Figure 10. Then this force will generate an additional horizontal component force due to the inclination angle θ of the bottom surface of the cone, which will lead to the risk of horizontal sliding much more likely. Based on this, to optimize the design of generic spindle-shaped spudcan structure, on the premise of retaining the anti-skidding cone tip at the bottom, the bottom part of the inverted cone is removed to make the bottom flat and so it only bears the vertical resistance, that is, a flat-bottomed spudcan, as shown in Fig. 11. Another way of reducing the horizontal sliding force induced on the right side of the spudcan is to adopt a concave-shaped style, as shown in Fig. 12. In this case, the horizontal resistance of

the soil generated on the bottom surface of the spudcan will counteract some horizontal sliding force generated on the right side of the spudcan, which can reduce the horizontal sliding force effectively. Besides, to assess the influence of the angle θ_1, there are two angles of 0° and 18.4° selected to carry out comparative analyses herein, that is the flat bottom shaped spudcan shown in Fig. 11 and the concave-shaped spudcan with the angle θ_1 of 18.4° shown in Fig.12. Besides, considering solid body will increase the difficulty of penetrating, 6 holes with a diameter of 2.7m were set to alter the generic spundcan. In view of the difficulty to extract with a cone shaped top, intercepting the curve of the obtuse end of the eggshell and replacing the conical surface of the generic spudcan, then a new type of spudcan structure generating less extracting resistance can be obtained, which is named as a lotus-shaped with 6 hole spudcan, as shown in Fig. 13.
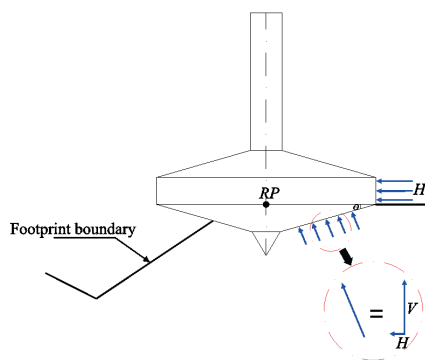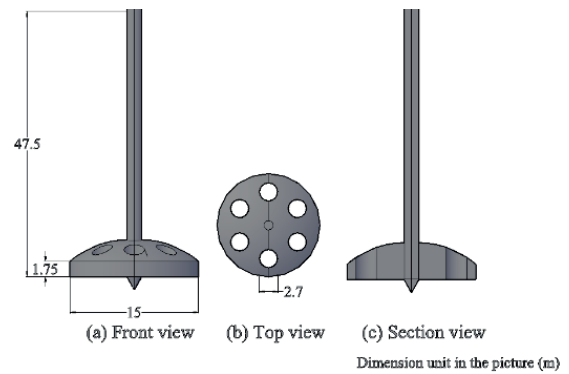

Fig. 13. Diagram of the lotus-shaped spudcan

COMPARATIVE ANALYSES OF DIFFERENT NOVEL SPUDCANS

PERFORMANCES OF DIFFERENT SHAPE SPUDCANS

Fig. 14 shows a comparison of the distribution of the vertical reaction force V, the horizontal sliding force H and the bending moment M along the penetration depth Z of the above mentioned four types of spudcans during penetrating near an existing footprint with an eccentric distance of 0.5D, that is, the generic spindle-shaped spudcan, the lotus-shaped spudcan with six holes, the flat-bottomed spudcan and the concave-shaped spudcan. In general, it indicates that the vertical reaction force V of the lotus-shaped spudcan is basically similar to that of the generic spindle-shaped spudcan, and those of the flat-bottomed spudcan and the concave-shaped spudcan are lightly larger than them relatively. In terms of horizontal sliding force H and bending moment M at RP_1, it shows that the results of the spindle-shaped spudcan are much larger than those of the other three types of spudcans. It all indicates that the proposed novel spudcans can mitigate the spudcan-footprint interactions effectively.

In order to intuitively reflect the relative variation rate of V, H, M induced to three kinds of novel spudcans compared with the generic spindle-shaped spudcan and the differences of in-place stability in the process of the spudcan penetrating, based on the obtained results shown in Fig. 14, the maximum horizontal sliding force H and the maximum bending moment at the top reference point PR_1 of the pile leg and their relative variation rate were calculated in Table 2. The statistical results show that, in the same conditions, compared with the generic one, the maximum horizontal sliding force H and the maximum bending moment at the top point PR_1 of the pile leg induced to three new types of the spudcan are decreased by 32.59%, 22.47%, 28.18% and 26.32%, 12.88%, 18.02% respectively. It can be seen that all three new types of spudcans can effectively reduce the adverse effects of spudcan-footprint interactions.
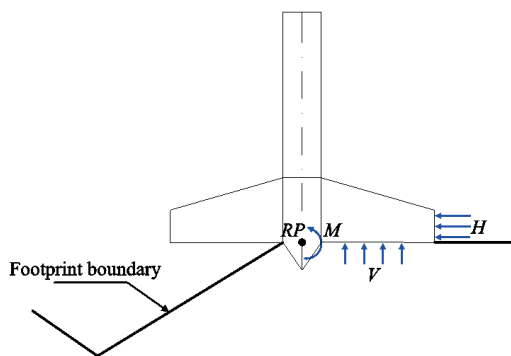

Fig. 10. Diagram of force mechanism of the generic spudcan

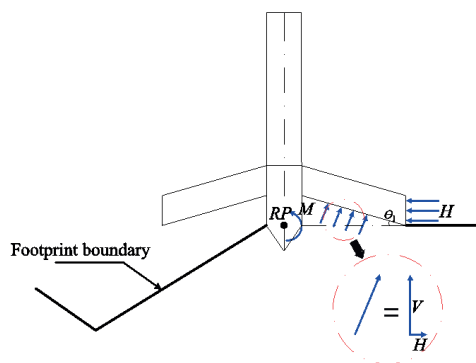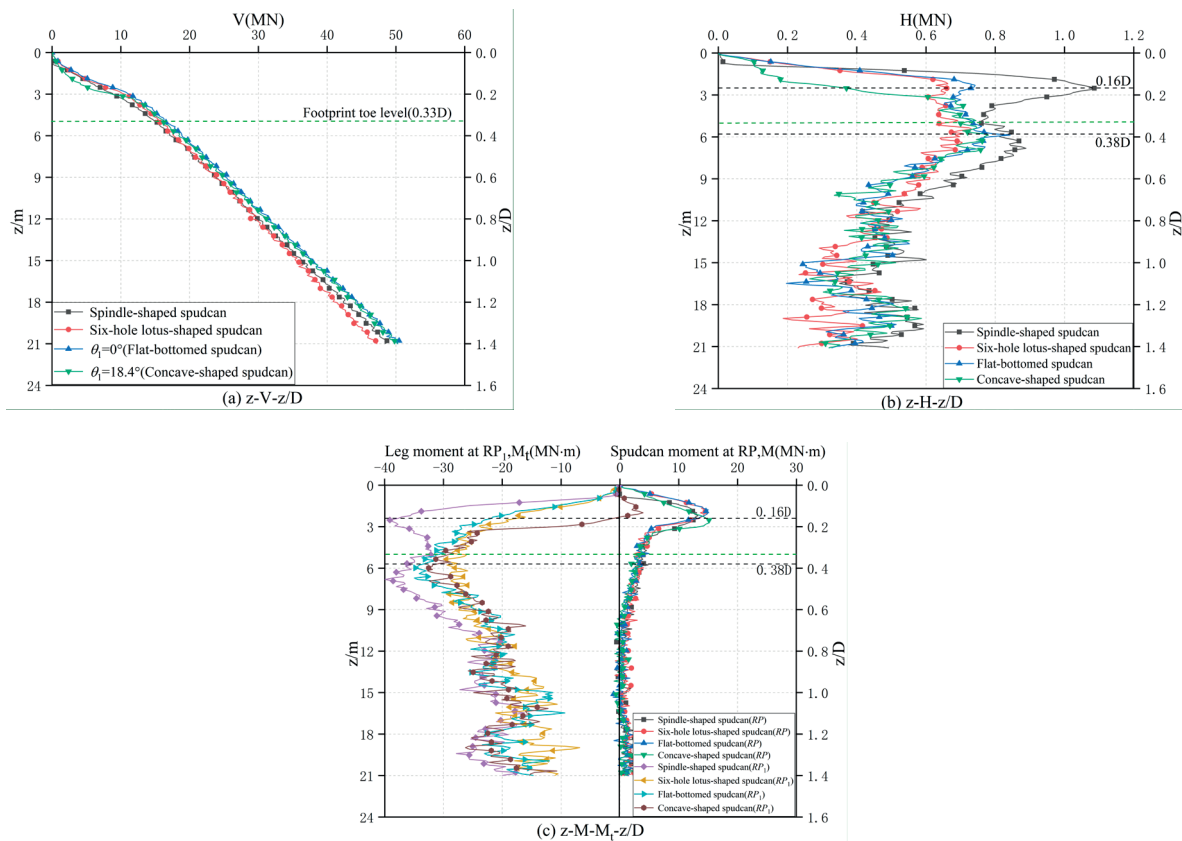*Fig. 11. Diagram of force mechanism of the flat bottom spudcan*

Fig. 12. Force mechanism of the concave-shaped spudcan

Fig. 14. Comparison of V, H, M of the four types of spudcans during reinstallation

Tab. 2. Horizontal sliding force of spudcan and change of bending moment at the top of pile leg

Types of spudcan	H(MN)	The variation rate of H_{max}	M_t(MN $\cdot$ m)	The variation ratio of M_{max}
Spindle-shaped	1.086	/	-39.899	/
Six-hole lotus-shaped	0.732	-32.59%	-29.398	-26.32%
Flat-bottomed	0.842	-22.47%	-34.761	-12.88%
Concave-shaped	0.780	-28.18%	-32.708	-18.02%

VARIATION LAW OF SOIL PLASTIC DEFORMATION IN HORIZONTAL RANGE

In order to directly reflect differences in the plastic deformation on both sides of soil foundations for the above mentioned four kinds of spudcans in the process of penetrating near an existing footprint, diagrams of plastic deformation of soil foundations with different penetrating depths (0.38D, 0.6D, 1D, 1.5D) were shown in Fig. 15. For comparing differences in soil disturbed zone in the horizontal range, statistics of the maximum horizontal range of soil plastic deformation on the left and right sides of the spudcan were shown in Fig. 16 with the penetrating depth of 0.38D, 0.6D, 1D and 1.5D respectively.

(a)the generic spudcan   (b)lotus-shaped spudcan   (c)flat-bottomed spudcan   (d)concave-shaped spudcan
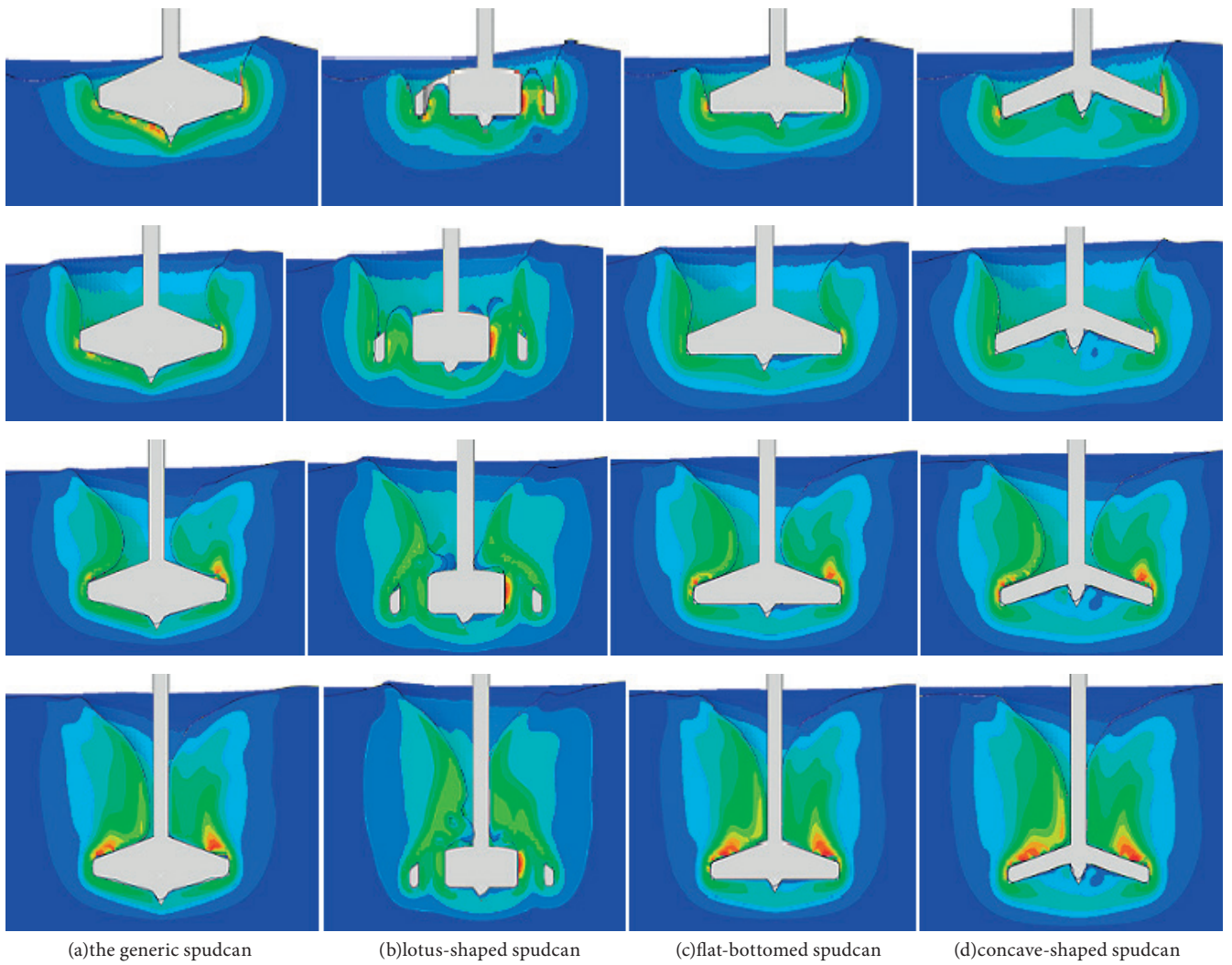
Fig. 15. Plastic deformation of soil during the process of spudcan reinstalling
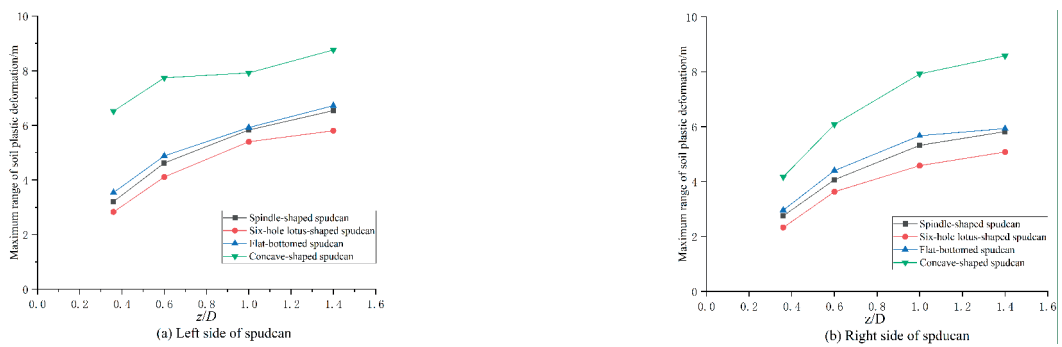
Fig. 16. Maximum horizontal range of plastic deformation for the four different kinds of spudcans

Type of spudcans	Maximum horizontal range of plastic deformation on the left side/m	Variation Ratio	Maximum horizontal range of plastic deformation on the right side /m	Variation Ratio
Spindle-shaped	6.54	/	5.82	/
Six-hole lotus-shaped	5.80	-11.32%	5.08	-12.71%
Flat-bottomed	6.72	+2.75%	5.93	+1.89%
Concave-shaped	8.76	+33.94%	8.58	+47.42%

As seen from Fig.16, the maximum horizontal range of plastic deformation of soil foundations on the left and right sides of the concave-shaped spudcan is greater than that of the generic one. At the completion of penetrating, the difference of the maximum horizontal range of plastic deformation of soil foundations for the two types of spudcans reaches the largest. Compared with the traditional spindle-shaped spudcan, differences on the left and right sides of the concave-shaped spudcan are increased by 33.94% and 47.42% respectively. However, the maximum horizontal range of plastic deformation of soil foundations on both sides of the lotus-shaped spudcan with six holes is smaller than that of the generic spindle-shaped spudcan, and compared with the generic one, differences on the left and right sides of the lotus-shaped spudcan with six holes are reduced by 11.32% and 12.71%, respectively. There are large differences between the asymmetry of soil foundations and the maximum horizontal range of plastic deformation of soil foundations on both sides of the above mentioned four types of spudcans with the penetrating depth of 0.38D, the reason is that when the lotus-shaped spudcan with six holes penetrating the soil foundation, part of the soils squeezed by the flat-bottom surface flowing into holes, which reduces the horizontal sliding range of soil. However, due to the existence of a concave cavity below the bottom of the concave-shaped spudcan, the soil under the action of squeezing needs to fill the cavity and then flow to the sides of the spudcan, which increases the horizontal sliding range of soil. In short, the maximum horizontal range of plastic deformation of soil foundation on both sides of the lotus-shaped spudcan with six holes is smaller than those of the other three kinds of spudcans, and the flat-bottomed spudcan is in the middle.

COMPARATIVE ANALYSES OF THE INCLINATION ANGLE AND THE OFFSET DISTANCE

In order to intuitively contrast variation tendencies of mechanical characteristics of a spudcan and pile legs among the three kinds of novel spudcans and the generic spindle-shaped spudcan, based on V, H, M curves of all kinds of spudcans in the process of penetrating, two standardized parameters, that is, the inclination angle of $\alpha = \tan^{-1}(H/V)$ and the offset distance of pile legs of $\delta = Mt/V$ were introduced to reflect the spudcan- footprint interaction, as shown in figure 17. And the comparison of the inclination angle α and the offset distance δ of all spudcans after anti-skidding cone submerged by the soil completely were shown in Table 4. It indicates that all three new types of a spudcan can reduce the inclination angle and the offset distance to some extent, and compared with the traditional spindle-shaped one, the lotus-shaped spudcan with six holes can reduce the maximum offset distance by 60.53%, the concave-shaped spudcan can reduce the maximum inclination angle by 66.57%. Therefore, compared with the generic spudcan, the three new types can reduce the sliding risk of the spudcan in the operation of jack-up rigs next to the existing footprint, meanwhile, increase the in-place stability of the spudcan obviously, which can provide a reference for the design of the spudcan structure of jack-up rigs.
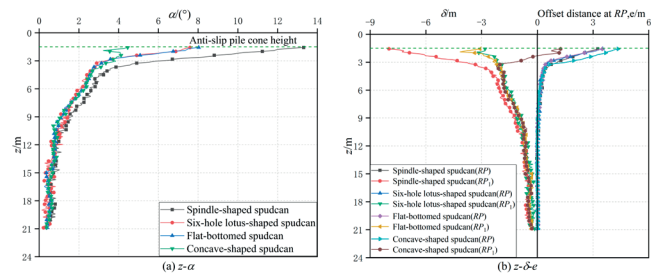
Fig. 17. Comparison of the inclination angle α and the offset distance δ of all spudcans

Tab. 4. Comparison of the inclination angle α and the offset distance δ of all spudcans

Type of spudcans	α/(°)	Variation rates of the inclination angle (α)	$|\delta|$/m	Variation rates of the offset distance $|\delta|$
Spindle-shaped spudcan	13.31	/	7.98	/
Six-hole lotus-shaped spudcan	7.59	-42.98%	3.15	-60.53%
Flat-bottomed spudcan	8.03	-39.67%	3.82	-52.13%
Concave-shaped spudcan	4.45	-66.57%	3.45	-56.76%

COMPARATIVE ANALYSES OF DIFFERENT MEASURES IN EASING SPUDCAN-FOOTPRINT INTERACTION

Currently, there are several measures presented in the literature to reduce consequences of spudcan-footprint interactions, such as stomping in advance, perforation drilling near the existing footprint and so on. In order to analyze merits and demerits of different kinds of measures, the spudcan shape optimization method proposed in this

paper, stomping in advance, and perforation drilling near the existing footprint were analyzed and compared based on CEL to discuss the application conditions of them.

STOMPING

The so-called "Stomping" means stomping in advance is performed outside the dangerous area near the existing footprint before the reinstalling of a spudcan to make the surrounding soils squeezed into the existing footprint, or to make the soils near the existing footprint pressed to the same depth as the bottom of the footprint, so as to level the seabed and reduce the horizontal sliding force. In this section, the eccentric distance of 0.5D was taken as the final position to reinstall the spudcan near an existing conical footprint as described earlier. The center distance of 0.75D, 1.00D, 1.25D, 1.50D, 1.75D and 2.00D were selected respectively to stomp with the stomping depth of 5m. The deformation of soil foundation with different center distances after spudcan stomping in advance and the final position of the spudcan penetrating were shown in Fig. 18. The parameters of the numerical calculation model were set in accordance with the previous.
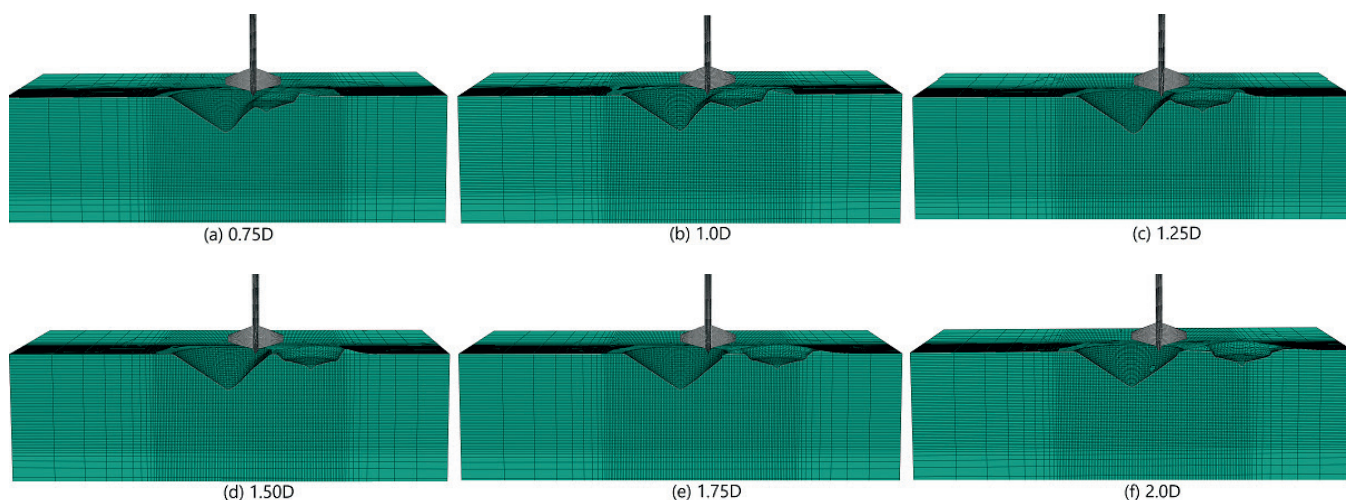
of perforation drilling near footprint scheme, Hossain et al. [32] put forward some useful suggestions: the ratio of drill diameter to the spudcan diameter should be 0.047-0.065, or the ratio of effective drilling diameter to the spudcan diameter should be 0.059~0.094. Distance between borehole center and adjacent borehole center should be 0.099~0.15. The area drilled in the perimeter of the spudcan should account for 13%~60% of the maximum vertical projection area of the spudcan.

In this section, the eccentric distance of 0.5D was taken as the final position to reinstall the spudcan near an existing conical footprint as described earlier as well. Based on the numbers of drilling holes, diameter and depth of boreholes set in the research of foundation drilling modeled by Pan et al. [33], the soil foundation near the projected perimeter of a spudcan was drilled in this study. The relevant working conditions were shown in Table 5. The number and layout of boreholes in soil foundation, the projected perimeter of the spudcan and the area of footprint were shown in Fig. 19. The setting of other parameters of the finite element model was consistent with the previous model, and 1/2 symmetric model was established for this research.

(a) 0.75D (b) 1.0D (c) 1.25D

(d) 1.50D (e) 1.75D (f) 2.0D

Fig. 18. Stomping in advance with different center distances

PERFORATION DRILLING

The so-called "Perforation Drilling " refers to presetting a certain number of hollow holes artificially in the soil along the perimeter of the spudcan, so as to reduce the adverse effect of the existing footprint when it penetrates near an existing footprint. Hossain and Stainforth [31] have conducted preliminary research on the perforation drilling scheme through a centrifugal test, and the effectiveness of this method in reducing the horizontal sliding risk of a spudcan during reinstallation near an existing footprint was verified. Although this method has not been used in practical engineering, the feasibility of this method to reduce the risk of puncture in stratified clay has been confirmed. For the relevant parameters

Tab. 5. Setting of conditions for perforation drilling of soil foundations

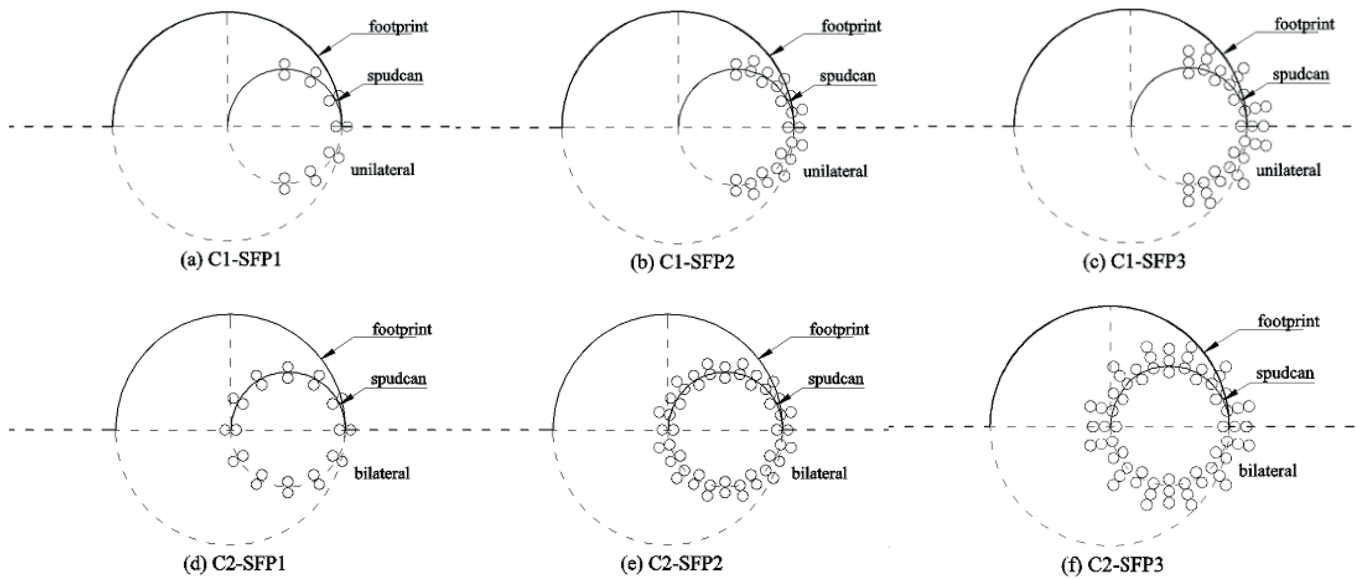| Conditions	Drilling diameter/m	Drilling depth/m	Drilling number	Drilling location
C1-SFP1	0.092D	$2Z_F$	24	unilateral
C1-SFP2	0.092D	$2Z_F$	48	unilateral
C1-SFP3	0.092D	$2Z_F$	64	unilateral
C2-SFP1	0.092D	$2Z_F$	24	bilateral
C2-SFP2	0.092D	$2Z_F$	48	bilateral
C2-SFP3	0.092D	$2Z_F$	64	bilateral

Fig. 19. Diagram of perforation drilling

COMPARISON ANALYSES OF THREE MEASURES TO MITIGATE SPUDCAN-FOOTPRINT INTERACTION

In order to intuitively compare the effectiveness of the above three types of measures in reducing the additional response generated by interactions of the spudcan-footprint, that is, the novel lotus-shaped spudcan with six holes, the stomping method and the perforation drilling method. In this study, comparison of variation rates of parameters V_{max}, H_{max} and M_{max}, which reflect the mechanical characteristics of the spudcan, and parameters α_{max} and δ_{max}, which reflect in-place stability of the spudcan, were comparatively analyzed with the penetrating depth of 10 m, as shown in Table 6. From the results in Table 6, it can be seen that, compared with the generic spindle-shaped spudcan without any dealing with the soil foundations in advance, the maximum value of horizontal sliding force and the maximum value of bending moment at the reference point of RP1 of the pile leg after stomping in advance with a distance from the center of 1.25D were reduced by 29.47% and 29.17%, and after perforation drilling with 64 holes unilateral in advance were reduced by 34.70% and 37.70%, and they have been effectively reduced

for lotus-shaped spudcan with six holes as well, with the rates of 21.45% and 16.19% , a slightly less than another two measures. For the inclination angle α and the offset distance of the pile leg δ, all three measures can lightly reduce the inclination angle but largely reduce the offset distance, with the maximum reduction rate of 50.46% for perforation drilling measures.

It can be seen that all above three measures can mitigate adverse effects caused by interactions of the spudcan-footprint effectively, and can greatly improve the stability of the spudcan when penetrating as well. Among them, according to the effect of reducing the additional stress of the spudcan, the effectiveness of them can be listed as follows: Perforation drilling near an existing footprint > the lotus-shaped spudcan with six holes > Stomping. While considering the vertical bearing capacity of a spudcan, the lotus-shaped spudcan with six holes improve it as much as 16.33% compared with the spindle-shaped structure due to the particularity of the structure, while because of reducing the continuity and strength of soil foundations, the perforation drilling measure leads to the decrease of the vertical bearing capacity of the spudcan by 13.07%.

Tab. 6. Comparisons of maximum and variation rate of related parameters of three measures

Conditions	V_{max}(penetrating depth 10m)/MN	Variation rate	H_{max}/MN	Variation rate	M_{tmax}/ MN·m	Variation rate	α_{max}/°	Variation rate	δ_{max}/°	Variation rate
Generic spudacan	19.728	\	2.072	\	-83.019	\	21.768	\	-14.201	\
Lotus-shaped spudcan	22.950	+16.33%	1.628	-21.45%	-69.576	-16.19%	14.556	-33.13%	-7.347	-48.26%
Stomping-1.25D	19.805	+0.3%	1.462	-29.47%	-58.803	-29.17%	14.502	-33.38%	-10.109	-28.81%
Drilling-C1-SFP3	17.149	-13.07%	1.353	-34.70%	-51.718	-37.70%	14.730	-32.33%	-7.035	-50.46%

In a word, the measure to optimize the spudcan shape, such as the new lotus-shaped spudcan with six holes, can ensure the vertical bearing capacity of the spudcan and can better suit for reinstalling near an existing footprint to improve the in-place stability. However, the existence of the holes in the spudcan structure increases the complexity of the structure shape and also increases the difficulty to produce it relatively, while the flat-bottomed spudcan and the concave-shaped spudcan are not bound by such limitations and can effectively mitigate interactions of the spudcan-footprint as well. Besides, although this kind of measure can well reduce interactions of the spudcan-footprint theoretically, it has not been verified in an actual condition. For stomping, the additional stress on the spudcan can be reduced in some extent after stomping in advance theoretically. However, in the actual working conditions, due to the complex marine soil foundation conditions and coverage by thick silt soil, the location and scale of the existing footprint are difficult to recognize, hence it is difficult to determine the position and depth of the stomping. Besides, if there is a fixed platform near the footprint, it may not be possible to conduct stomping in the ideal position, and if the new jack-up rig spudcans are used in stomping operation, the jack-up rig structure also has some risks of instability if the foundation conditions are too poor and the time of the loading pump is too long. For perforation drilling near an existing footprint, in theory, it also can reduce the additional stress acting on the spudcan in some extent, but this scheme has not been implemented in practical engineering either. Perforation drilling method can decrease additional stress acting on the spudcan by means of an adjusting strength of the soil on both sides of the spudcan through drilling, but this scheme changes the integrity of the soil and reduces the bearing capacity of the soils below the spudcan projection. Therefore, if it is necessary to ensure the in-place stability of a jack-up rig structure, there is a need to increase the depth of the spudcan penetrating or employ some related foundation reinforcement measures. Moreover, due to the complex marine soil foundation conditions and coverage by thick silt soil in the actual working conditions, the perforation drilling location of soil foundation is more difficult to be selected and the depth of drilling is more difficult to be determined. In addition, the selection of perforation drilling parameters for different craters is quite a discrepancy, and the relevant drilling equipment needs to be prefabricated in advance, but the universality of drilling instruments is poor, so these measures will significantly increase the construction cost.

In brief, it can be concluded that all the three measures have merits and demerits, so the relevant construction environment conditions and engineering practice should be fully considered when selecting measures to deal with interactions of the spudcan-footprint.

CONCLUSIONS

This paper discussed possible measures to mitigate spudcan-footprint interactions when a jack-up rigs reinstalling near an existing footprint. Based on the mechanical mechanism of a spudcan, three novel spudcan shapes were proposed, and mechanical characteristics of these novel spudcans and a flow mechanism of soil foundations were investigated comparatively. Besides, three types of possible measures for easing spudcan-footprint interactions were analyzed comparatively as well. Conclusions from this study are as follows:

1. In comparison with the generic spindle-shaped spudcan, the lotus-shaped spudcan with six holes, the flat-bottomed spudcan, and the concave-shaped spudcan can reduce the horizontal sliding force and the bending moment at the top of the pile leg by 32.59%, 22.47%, 28.18%, and 26.32%, 12.88%, 18.02%, respectively, which indicates that all three novel spudcan can reduce adverse consequences during reinstallation of the spudcan near an existing footprint effectively.

2. During reinstallation of the spudcan near an existing footprint, the horizontal range of plastic deformation of the disturbed soil generated by the flat-bottomed spudcan and the concave-shaped spudcan is larger than the generic ones, and that of the lotus-shaped spudcan with six holes is less than that generated by the generic one.

3. Two normalized parameters, the inclination angle of the spudcan α and the offset distance of the pile leg   are introduced to reflect consequences induced by interactions of the spudcan-footprint. The results show that all three new types of spudcans can reduce inclination angle of the spudcan and offset distance of the pile leg effectively, and in comparison with the generic one, the inclination angle of the lotus-shaped spudcan is 60.53% less than that of the generic spindle-shaped spudcan, and the inclination angle of the concave-shaped spudcan is 66.57% less than that of the generic one.

4. Three possible measures in mitigating interactions of the spudcan-footprint were contrasted, that is the novel spudcan (represented by the lotus-shaped spudcan with six holes), stomping method, perforation drilling method. The results show that all of them can reduce adverse consequences induced by interactions of the spudcan-footprint, and also can improve the in-place stability of the spudcan during reinstallation. In addition, according to the effect of reducing the additional stress of the spudcan, the effectiveness of them can be listed as follows: perforation drilling near an existing footprint > the lotus-shaped spudcan with six holes > stomping. While considering the vertical bearing capacity of the spudcan, the lotus-shaped spudcan with six holes improve it as much as 16.33% compared with the spindle-shaped structure due to the particularity of the structure, while because of reducing the continuity and strength of soil foundations, the perforation drilling measure leads to the decrease of the vertical bearing capacity of the spudcan by 13.07%. It can be concluded that all three measures have merits and demerits, so the relevant

construction environment conditions and engineering practice should be fully considered when selecting measures to deal with interactions of the spudcan-footprint.

REFERENCES

1. Clarom, in: P. Le Tirant, C. Pérol (Eds.), Design guides for offshore structures, Club des Actions de Recherche sur les Ouvrages en Mer, Paris, 1993.

2. M.F. Randolph, M.J. Cassidy, S. Gourvenec and C.J. Erbrich, "Challenges of offshore geotechnical engineering", Proceedings of the 16th International Conference on Soil Mechanics and Geotechnical Engineering: Geotechnology in Harmony with the Global Environment, 2005, Vol. 1, 123-176.

3. M.S. Hossain, R. Stainforth, V.T. Ngo, M.J. Cassidy, Y.H. Kim and M.J. Jun, "Experimental investigation on the effect of spudcan shape on spudcan-footprint interaction", Applied Ocean Research, 2017. Vol. 69, 65-75, doi: 10.1016/j.apor.2017.10.003

4. M.J. Jun, Y.H. Kim, M.S. Hossain, et al., "Numerical investigation of novel spudcan shapes for easing spudcan-footprint interactions", Journal of Geotechnical and Geoenvironmental Engineering, 2018. Vol. 144(9), 04018055, doi: 10.1061/(ASCE)GT.1943-5606.0001925

5. C.T. Gan, C.F. Leung, M.J. Cassidy, C. Gaudin and Y.K. Chow, "Effect of time on spudcan-footprint interaction in clay", Geotechnique, 2012. Vol. 62(5), 401-413, doi: 10.1680/geot.10.P.063

6. J.J. Osborne, "Are we good or are we lucky?", OGP/CORE Workshop, Singapore, 2005.

7. R.L. Jack, M.J.R. Hoyle, N.P. Smith and R.J. Hunt, "Jack-up accident statistics –A further update", Proceedings of the 14th International Conference on the Jack-up Platform Design, Construction and Operation, London, 2013.

8. R.J. Hunt and P.D. Marsh., "Opportunities to improve the operational and technical management of jack-up deployments", Marine Structures, 2004. Vol. 17 (3–4), 261–273, doi: 10.1016/j.marstruc.2004.08.005

9. B. Van den Berg, B. Hulshof, T. Tijssen and P. Van Oosterom, "Harmonisation of distributed geographic datasets: a model driven approach for geotechnical & footprint data", Delft: Delft University of Technology, 2004.

10. M.S. Hossain and X. Dong, "Extraction of spudcan foundations in single and multilayer soils", Journal of Geotechnical and Geoenvironmental Engineering, 2014. Vol. 140(1), 170–184, doi: 10.1061/(ASCE)GT.1943-5606.0000987

11. V.W. Kong, M.J. Cassidy and C. Gaudin, "Experimental study of the effect of geometry on reinstallation of jack-up next to footprint", Canadian Geotechnical Journal, 2013. Vol. 50(5), 557–573, doi: 10.1139/cgj-2012-0381

12. V.W. Kong, M.J. Cassidy and C. Gaudin, "Failure mechanisms of a spudcan penetrating next to an existing footprint", Theoretical and Applied Mechanics Letters, 2015. Vol. 5(2), 64–68, doi: 10.1016/j.taml.2014.12.001

13. R.J. Jardine, N. Kovecevic, M.J.R. Hoyle, H.K. Sidhu and Letty A, "Assessing the effects on jack-up structures of eccentric installation over infilled craters", Proceeding of Offshore Site Investigation and Geotechnics, Diversity and Sustainability, 2002, 307–324.

14. D.F. Hartono, C.F. Leung, K.K. Tho and Y.K. Chow, "Centrifuge and numerical modelling of reaming as mitigation measure for spudcan footprint interaction", Proceedings of 2014 Offshore Technology Conference, 2014.

15. A. Grammatikopoulou, R.J. Jardine, N. Kovacevic, D.M. Potts, M.J.R. Hoyle and K.M. Hampson, "Potential solutions to the problem of the eccentric installation of jack-up structures into old footprint craters", Proceeding of Offshore Site Investigation and Geotechnics Conference, Confronting New Challenges and Sharing Knowledge, 2007, 293–300.

16. R. Brennan, H. Diana, R.W.P. Stonor, M.J.R. Hoyle, C.P. Cheng, D. Martin and R. Roper, "Installing jack-ups in punch through- sensitive clays", Proceeding of Offshore Technology Conference, 2006.

17. P. Handidjaja, C.T. Gan, C.F. Leung and Y.K. Chow, "Jack-up foundation performance over spudcan footprints analysis of a case history", Proceeding of 12th International Conference on the Jack-up Platform Design, 2009.

18. M.J. Jun, Y.H. Kim, M.S. Hossain, Y. Hu and S.G. Park, "Global jack-up rig behaviour next to a footprint", Marine Structures, 2019. Vol. 64, 421-441, doi: 10.1016/j.marstruc.2018.12.002

19. M.J. Jun, Y.H. Kim, M.S. Hossain, M.J. Cassidy, Y. Hu and S.G. Park, "Geotechnical centrifuge investigation of the effectiveness of a novel spudcan in easing spudcan-footprint interactions", Journal of Geotechnical and Geoenvironmental Engineering, 2020, Vol. 146(8), 04020071, doi: 10.1061/(ASCE)GT.1943-5606.0002322

20. M.S. Hossain and M.F. Randolph, "Effect of strain rate and strain softening on the penetration resistance of spudcan foundations on clay", International Journal of

Geomechanics, 2009, Vol. 9(3), 122–132, doi: 10.1061/(ASCE)1532-3641 (2009)9:3(122)

21. Simulia, Abaqus 6.10 Online Documentation. Dassault Systems Simula Corp., Providence, RI, USA, 2014.

22. G. Qiu and S. Henke, "Controlled installation of spudcan foundations on loose sand overlying weak clay", Marine Structures, 2011. Vol. 24(4), 528–550, doi: 10.1016/j.marstruc.2011.06.005

23. K.K. Tho, C.F. Leung, Y.K. Chow and S. Swaddiwudhipong, "Eulerian finite-element technique for analysis of jack-up spudcan penetration", International Journal of Geomechanics, 2012. Vol. 12(1), 64–73, doi: 10.1061/(ASCE) GM.1943-5622.0000111

24. J. P. Michalski, "Parametric Method Applicable in Assessing Breakout Force and Time for Lifting Slender Bodies from Seabed," Polish Marit. Res., vol. 27, no. 2, 2020, doi: 10.2478/pomr-2020-0028

25. J. Zheng, M.S. Hossain and D. Wang, "Numerical modeling of spudcan deep penetration in three-layer clays", International Journal of Geomechanics, 2015. Vol. 15(6), 04014089, doi: 10.1061/(ASCE) GM.1943-5622.0000439

26. P. Hu, D. Wang, M.J. Cassidy, S.A. Stanier, "Predicting the resistance profile of a spudcan penetrating sand overlying clay", Canadian Geotechnical Journal, 2014, Vol. 51(10), 1151-1164, doi: 10.1139/cgj-2013-0374

27. W. Zhang, M.J. Cassidy and Y. Tian, "3D large deformation finite element analyses of jack-up reinstallations near idealised footprints", Proceedings of the 15th International Conference on the Jack-Up Platform Design, 2015.

28. P. Gao, Z. Liu, J. Zeng, Y. Zhan, and F. Wang, "A Random Forest Model for the Prediction of Spudcan Penetration Resistance in Stiff-Over-Soft Clays," Polish Marit. Res., vol. 27, no. 4, 2020, doi:10.2478/pomr-2020-0073

29. MAO Dongfeng, ZHANG Minghui, ZHANG Laibin, et al. Sliding risk of jack-up platform re-installation close to existing footprint and its countermeasure[J]. Petroleum Exploration and Development, 2015, 42(2): 233-237

30. YU L, ZHANG H Y, LI J, et al. Finite element analysis and parametric study of spudcan footing geometries penetrating clay near existing footprints[J]. Journal of Marine Science and Engineering, 2019, 7(6): 175

31. M.S. Hossain and R. Stainforth, "Perforation drilling for easing spudcan-footprint interaction issues", Ocean Engineering, 2016. Vol. 113, 308-318, doi: 10.1016/j.oceaneng.2016.01.002

32. N.H.C. Chan, J.M. Paisley and G.L. Holloway, "Characterization of soils affected by rig emplacement and Swiss cheese operations-Natura Sea, Indonesia, a case study", Proceedings of the 2nd Jack-up Asia Conference and Exhibition, Singapore, 2008, 17-18.

33. D. Shi, G. Pan and Z.H. Liu, "Mitigation effect of perforation drilling on the sliding risk during spudcan installation close to footprints", Journal of Marine Science and Engineering, 2020. Vol. 8(2), 118, doi: 10.3390/jmse8020118

CONTACT WITH THE AUTHORS

Huafeng Yu
e-mail: yu_hf@ecidi.com

Zhenzhou Sun
e-mail: sun_zz@hdec.com

Linlin He
e-mail: helinl@126.com

Key Laboratory
of Far-shore Wind Power Technology
of Zhejiang Province
Gaojiao Road, Yuhang District, 311122 Hangzhou
China

Liu Yang
e-mail: YL181026@163.com

National Engineering Research Center
for Inland Waterway Regulation
Chongqing Jiaotong University
Xuefu Avenue, 400074 Chongqing
China